J. Physiol. (1979), **288**, *pp.* 613–634
With 10 *text-figures*
Printed in Great Britain

RESPONSES OF RETINAL RODS TO SINGLE PHOTONS

BY D. A. BAYLOR, T. D. LAMB* AND K.-W. YAU*

From the Department of Neurobiology,
Stanford University School of Medicine,
Stanford, California 94305, U.S.A.

(*Received 12 June 1978*)

SUMMARY

1. A suction electrode was used to record the membrane current of single rod outer segments in pieces of toad retina. During dim illumination the membrane current showed pronounced fluctuations.

2. Amplitude histograms of responses to dim flashes of fixed intensity exhibited two discrete peaks, one at 0 pA and one near 1 pA, suggesting that the response was quantized. By setting a criterion amplitude level, flash responses could be classed as 'failures' (no response) or as 'successes' (at least one quantal event).

3. The variation of fraction of successes with flash intensity was consistent with the hypothesis that each quantal electrical event resulted from a single photoisomerization.

4. The quantal event had a mean amplitude of about 1 pA (5% of the standing dark current) and a standard deviation of 0·2 pA. Dispersion in the event amplitude prevented identification of histogram peaks corresponding to two or more photoisomerizations.

5. Individual quantal responses exhibited a smooth shape very similar to that of the average quantal response. This suggests that a single photoisomerization releases many particles of transmitter and that radial diffusion of internal transmitter is not a major source of delay in the light response.

6. The 'quantum efficiency' with which an absorbed photon generated an electrical event was measured as $0{\cdot}5 \pm 0{\cdot}1$ (S.E. of mean, $n = 4$). This is slightly lower than the quantum efficiency of photoisomerization obtained previously for rhodopsin in solution.

7. At wavelengths between 420 and 700 nm the quantal event was invariant in size, although the cell's sensitivity varied over a range of 10^5.

8. The power spectrum of the fluctuations in dim steady light was predicted by assuming that a random series of quantal events occurred independently.

9. In brighter light the fluctuations were faster, and the response to an incremental flash was reduced in size and duration. The power spectrum could be predicted by assuming random superposition of events with the shape of the incremental flash response.

* Present address: Physiological Laboratory, University of Cambridge, Cambridge CB2 3EG.

INTRODUCTION

The previous paper (Baylor, Lamb & Yau, 1979) described general properties of the membrane current recorded from single toad rod outer segments. Here we examine fluctuations of the photocurrent in dim light and present evidence that they arise from the quantal nature of the stimulus. Responses to single photons are identified and certain features relevant to the visual transduction mechanism are investigated.

A preliminary report of some of this work has been published previously (Yau, Lamb & Baylor, 1977), and similar results have been obtained by R. N. McBurney and J. L. Schnapf (personal communication).

METHODS

Experiments were performed on single rod outer segments in the retina of the toad, *Bufo marinus*, using the methods of Baylor *et al.* (1979), with the following additions.

Quantum efficiency

Determination of the probability (quantum efficiency) with which an absorbed photon gives rise to an electrical response required accurate measurement of the fraction of incident photons absorbed by an outer segment. For this purpose, light collected by the microscope objective was diverted through the camera side-tube of the microscope to the photomultiplier of a quantum photometer (Princeton Applied Research, 1140 A/B). The discriminator output of the photometer was taken to a 100 MHz digital counter (Tektronix, DC501) and the linear analogue output to the tape recorder and chart recorder. The counter was set to count over a 10 sec period, during which the shutter in the optical beam was automatically opened. The dark count rate was about 25 counts sec^{-1}, and the light intensities used gave rates of about 5000 counts sec^{-1}. For a counting efficiency of 1 % and with 10 % fractional absorption, a measuring beam of this intensity and duration would be expected to bleach less than 0·1 % of the 10^9 pigment molecules in the rod.

The light stimulus was in the form of a narrow slit centred on and parallel to the long axis of the outer segment and not quite filling it (nominal width 2·5 μm, typical length 30 μm). The light was plane polarized with the electric vector normal to the long axis of the outer segment (i.e. in the 'preferred' direction) to obtain maximum absorption. To decrease absorption by the yellow photoproduct metarhodopsin III ($\lambda_{max} \simeq 465$ nm) while maintaining reasonably high absorption by rhodopsin ($\lambda_{max} \simeq 500$ nm) the test beam was at 520 nm. A reference 580 nm light, which is poorly absorbed by rhodopsin, was used as a check that transmission changes due to other factors did not occur.

The procedure was to first measure the mean number of quantal electrical events induced by dim 520 nm flashes. The light intensity was then increased and the transmitted flux was measured with the quantum photometer at 520 and 580 nm both before and 30–60 sec after the end of a bright 60 sec bleaching light. The fractional absorption and quantum efficiency of response generation were then determined. As discussed on p. 624 it was not possible to eliminate the effects of metarhodopsin III, and a correction was made.

Signal processing

Signals recorded on an FM tape recorder were replayed through a 6-pole low-pass filter with cut-off frequency set between 10 and 50 Hz. The filtered signals were digitized to 12-bit accuracy with a PDP-11/34 computer and stored on magnetic disk.

Power spectra. The power spectral density was computed using the methods outlined by Bendat & Piersol (1971, p. 327). Each data record, which usually consisted of 4096 or 2048 points sampled at 10 or 20 msec intervals (40·96 sec total), was cosine tapered. Raw spectral values were usually averaged over a number of frequency points to obtain final spectra.

Amplitude of response to dim flashes. In order to prepare amplitude histograms of responses to dim flashes, amplitudes were measured by a 'difference' and a 'least-squares' method. The

first method measured the difference between the signal level over a period near the peak and over a period before the flash, while in the second method the ensemble average response was scaled to provide a least-squares fit to each individual response.

Consider the responses $r_j(t)$, $j = 1, \ldots N$, to N presentations of a dim flash, and let the ensemble average be $\bar{r}(t)$. Consider three time windows, such as those labelled T_1, T_2, and T_3 in Fig. 4, and denote the time average of $r_j(t)$ over interval T_1 as $r_j(T_1)$, etc.

In the difference method the jth response amplitude r_j is defined as

$$r_j = r_j(T_2) - r_j(T_1), \tag{1}$$

where windows T_1 and T_2 are respectively before the stimulus and near the peak of the response.

The mean response amplitude for the N trials is

$$\mu = \bar{r}(T_2) - \bar{r}(T_1), \tag{2}$$

which may be considered either as the ensemble average of the r_j values; or as the difference in $\bar{r}(t)$ between periods T_1 and T_2.

In the least-squares method the ensemble average response $\bar{r}(t)$ is scaled by the factor a_j, in order to provide the least-squares fit to each individual response $r_j(t)$ over the period T_3. To minimize

$$S = \int_{T_3} \{r_j(t) - [a_j \bar{r}(t) + b_j]\}^2 \, dt \tag{3}$$

the partial derivative $\partial S/\partial a_j$ is set equal to zero, and this requires the dimensionless factor a_j to be

$$a_j = \frac{\int_{T_3} \{r_j(t) - r_j(T_3)\} \{\bar{r}(t) - \bar{r}(T_3)\} \, dt}{\int_{T_3} \{\bar{r}(t) - \bar{r}(T_3)\}^2 dt}, \tag{4}$$

(similar to the expression for the slope of a linear regression fit). The least-squares response amplitude r_j is then the scaled mean, or

$$r_j = a_j \mu. \tag{5}$$

In computing the response amplitude in this way both the individual response and the scaled ensemble average were displayed on an oscilloscope; visual inspection showed that in most cases a very good fit was obtained. Measurement of the response by the least-squares method is equivalent to the analog operation of passing the signal through a 'matched filter' (see Davenport & Root, 1958) before measuring its size.

The values of response amplitude r_j evaluated by the two methods (eqns. (1) and (5)) were in close agreement, and the associated amplitude histograms were very similar. Amplitudes and histograms given in this paper were obtained with the least-squares method but were also checked by the difference method.

RESULTS

Fluctuations in the response to steady light

Fig. 1 shows records of outer segment membrane current during steady illumination at a series of intensities. The bars beneath the traces indicate the duration of the stimuli and the numbers give the applied intensities in photons μm^{-2} sec^{-1}. The response to the dimmest light (bottom trace) consisted of a series of small transient components of outward membrane current. Each of these events had a rounded shape resembling that of the dim flash response and a peak amplitude of about 1 pA. At the next higher intensity (0·068 photons μm^{-2} sec^{-1}) the mean response was larger and the fluctuations were more pronounced. Further increases in light intensity gave larger mean responses, but the fluctuations decreased until at saturation (760 photons μm^{-2} sec^{-1}) they were absent. The similarity of these fluctuations to those previously observed in invertebrate photoreceptors (e.g. Fuortes &

Yeandle, 1964) suggests that they may result from the quantal nature of the light stimulus. To investigate this it is convenient first to analyse the response to dim flashes.

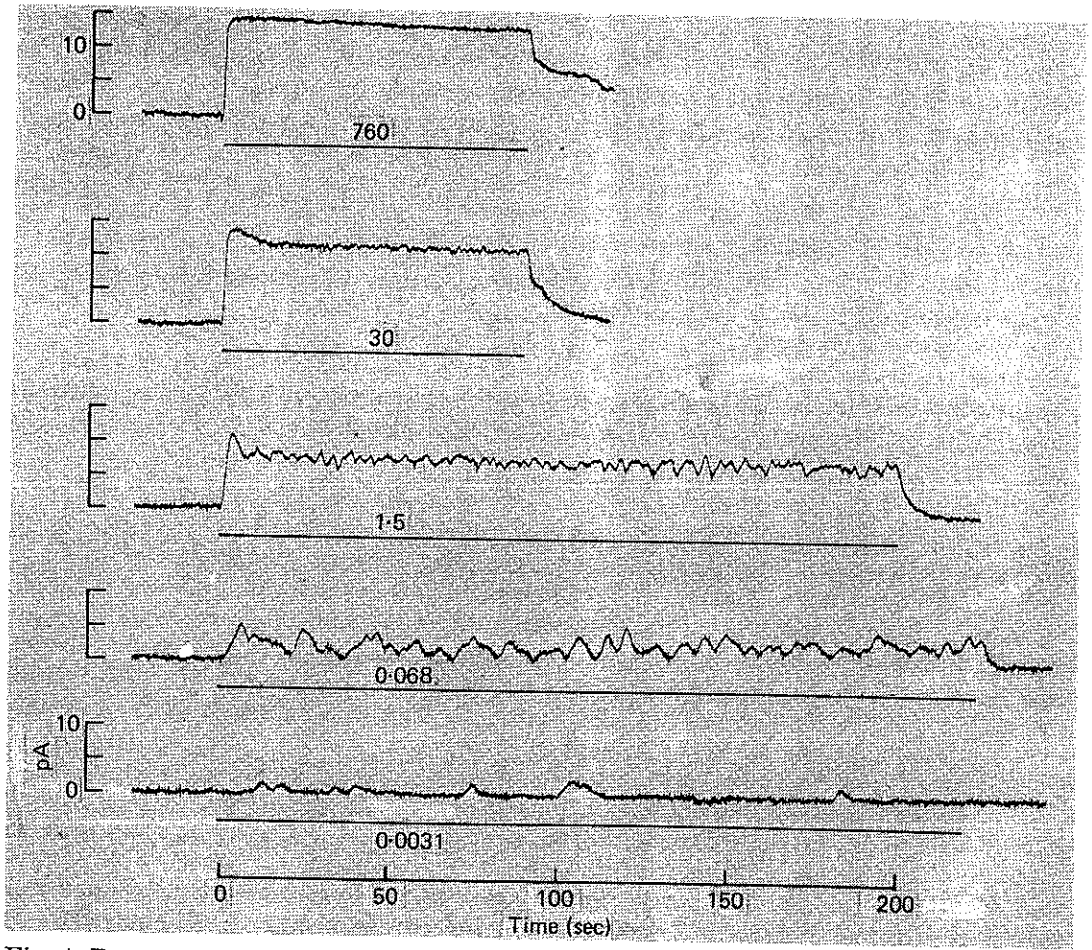

Fig. 1. Response of a rod outer segment to steady lights. Ordinate is outward change in membrane current from level in darkness. Bars beneath traces indicate duration of light stimuli; numbers give intensities in photons μm^{-2} sec^{-1}; 500 nm local light. Cell 1 of Table 1, cell 12 of Baylor *et al.* (1979) Table 1. Low-pass filtered at 15 Hz.

Analysis of fluctuation in flash responses

Previous intracellular records from toad rods have shown that responses to a series of identical flashes are all of very nearly the same size, even at intensities so low that the mean number of photons absorbed in an outer segment should be less than one (Fain, 1975). In contrast, membrane current responses showed considerable variation in amplitude, as illustrated in Fig. 2 for forty consecutive dim flashes. In several of the trials there was no apparent response, in others a small response of about 1 pA, and occasionally a larger response. This behaviour suggests that the flash response is quantized, as might be expected when on average very few photons are absorbed. The amplitude histogram for ninety-nine responses at this flash intensity is plotted in Fig. 3*A* and shows pronounced peaks at 0 pA and at 1–1·5 pA. On the assumption that the first non-zero peak corresponds to the occurrence of a unit (or quantal) event, it is possible to designate responses as 'successes' or 'failures' by setting a criterion level between the two peaks (arrow in Fig. 3*A*). Any response

larger than this is assumed to represent occurrence of at least one event (success), and any smaller response to represent the absence of events (failure). With a criterion level of 0·5 pA, it is estimated that fifty-eight of the ninety-nine trials in Fig. 3*A* resulted in failure. In Fig. 3*B*, from the same cell at a lower intensity, this criterion level indicated that forty-four of the fifty-two trials were failures.

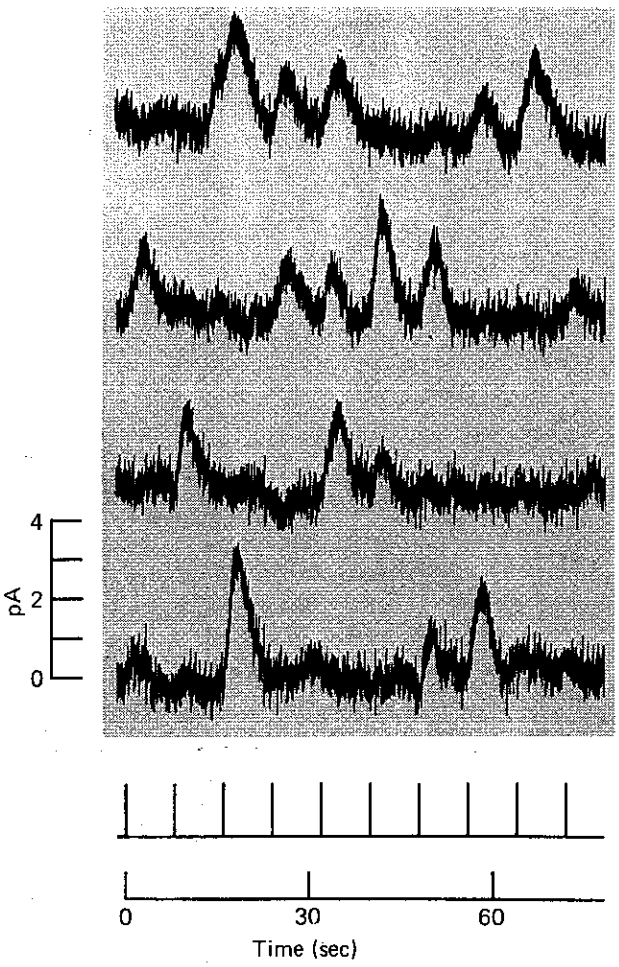

Fig. 2. Response of outer segment to a series of forty consecutive dim flashes. Local illumination; 20 msec flash delivering 0·029 photons μm^{-2} at 500 nm, flash timing monitored below; saturating response 12 pA. Same cell as Fig. 1. Low pass filtered at 30 Hz.

Mean number of unit events per flash

On the assumptions that the response is indeed quantized, and that occurrence of the underlying events is Poisson-distributed, then the probability p_k that there will be k events per trial is

$$p_k = \frac{e^{-m}m^k}{k!}, \tag{6}$$

where m is the mean number of events per trial. The probability of failure ($k = 0$) is simply

$$p_0 = e^{-m}, \tag{7}$$

so that for $p_0 = 58/99$ the mean number of quantal events per trial would be $m = 0{\cdot}53$.

Estimates of unit response amplitude

From form of histogram. An estimate of the unit amplitude, a, can be obtained most simply by inspection of the histogram and visual location of the centre of the first peak at non-zero amplitude. In Fig. 3*A* this appears to be close to 1·2 pA.

From μ and m. A second estimate of the event amplitude can be obtained from the

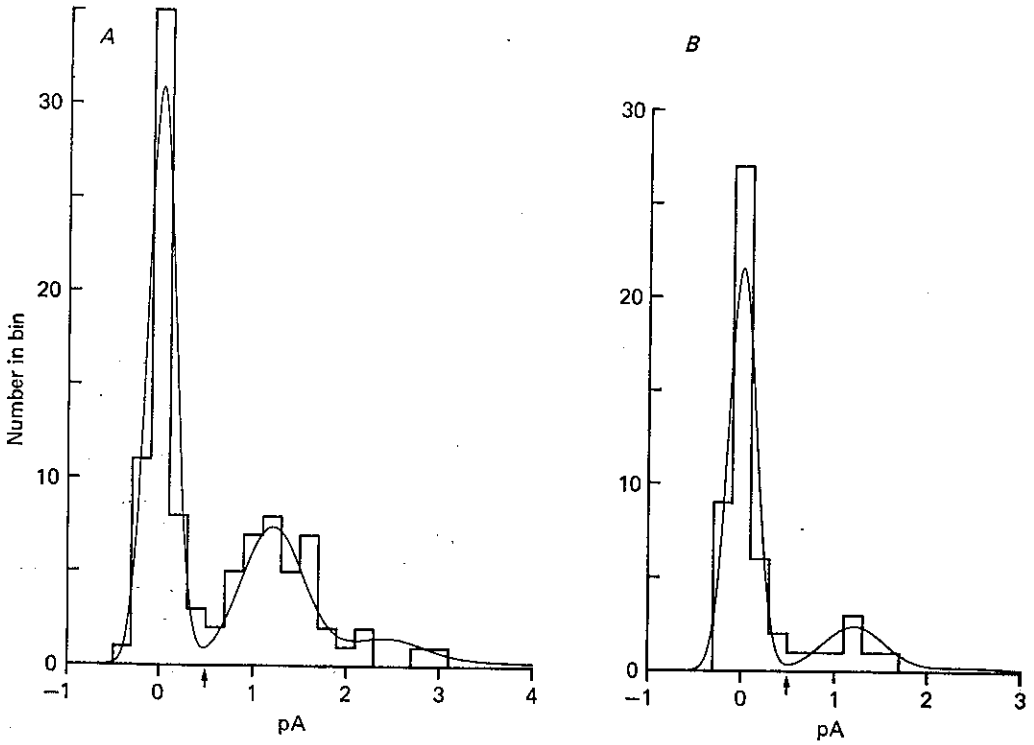

Fig. 3. Amplitude histograms for flash responses. Amplitudes were measured by the least squares method described on p. 614. Ordinate is number of occurrences of amplitude shown on abscissa, bin width 0·2 pA. *A*, from same cell and same flash intensity (0·029 photons μm^{-2}) as in Fig. 2; ninety-nine trials. Response amplitude had mean $\mu = 0{\cdot}56$ pA and variance $\sigma^2 = 0{\cdot}58$ pA^2. The curve is eqn. (10) with $m = 0{\cdot}53$, $a = 1{\cdot}2$ pA, $\sigma_0 = 0{\cdot}15$ pA and $\sigma_1 = 0{\cdot}3$ pA. *B*, same cell, lower intensity (0·014 photons μm^{-2}); fifty-two trials. Mean response $\mu = 0{\cdot}17$ pA, variance $\sigma^2 = 0{\cdot}21$ pA^2. Curve is for same parameters, except $m = 0{\cdot}25$. Arrows mark the criterion level of 0·5 pA used to separate responses from failures.

mean response amplitude, μ, and the mean number of events per trial, m, using the relation

$$\mu = ma. \tag{8}$$

The measured value of the mean response in Fig. 3 was 0·56 pA which with the above value of $m = 0{\cdot}53$ gives an amplitude of $a = 1{\cdot}06$ pA.

From the variance of the response. A third estimate of the unit amplitude can be obtained from the variance of the response, determined in either of two ways. The first method is to compute the variance of the response amplitudes measured in plotting the histogram (see Methods, p. 614); this gave a value of $\sigma^2 = 0{\cdot}58$ pA^2 for the responses used in obtaining Fig. 3*A*. The second method is to compute the ensemble variance at each instant of time after the flash, as was suggested by Baylor & Hodgkin (1973) and done for turtle rods by Schwartz (1975) and for turtle cones by

Lamb & Simon (1977). Fig. 4 is a plot of the average and variance of the responses used to obtain Fig. 3*A*; at the peak of the response there was a variance increase of $\sigma^2 = 0{\cdot}55$ pA^2, reasonably consistent with the value above.

Again assuming a Poisson distribution of events, the variance of the response amplitude should be related to the mean by

$$\sigma^2 = \mu a, \tag{9}$$

ignoring non-linearity and dispersion of quantal response sizes (see p. 620). For $\sigma^2 = 0{\cdot}58$ pA^2 and $\mu = 0{\cdot}56$ pA this method gives a value of $a = 1{\cdot}03$ pA.

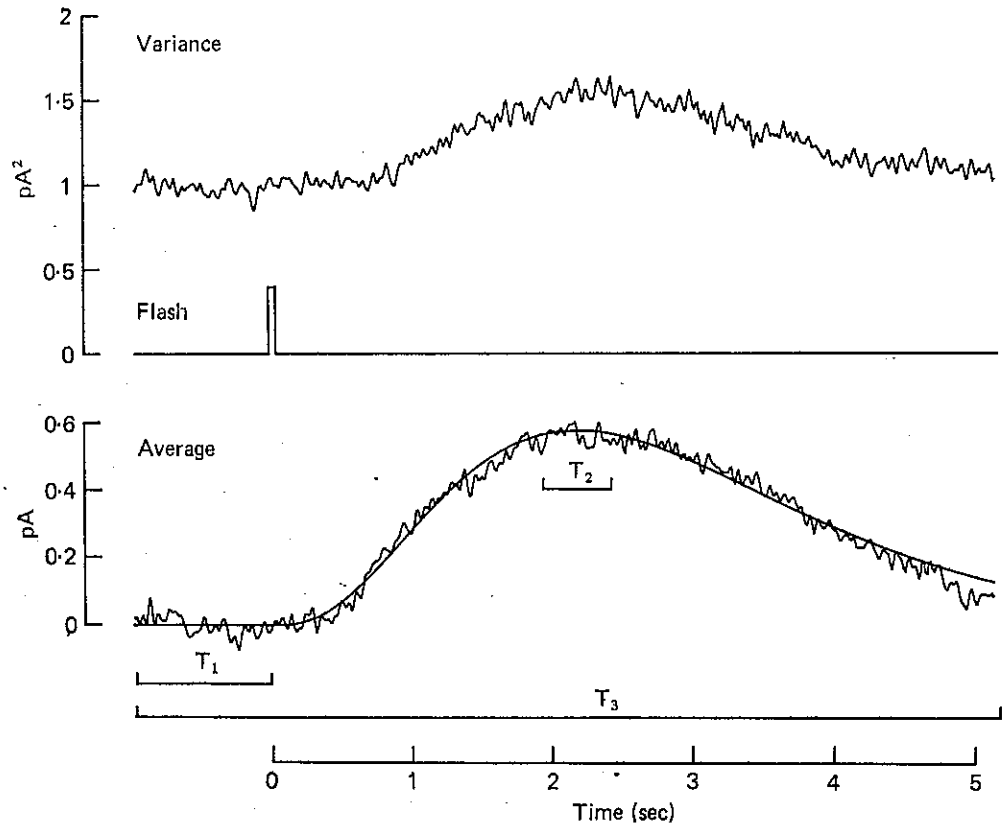

Fig. 4. Ensemble average and variance of the ninety-nine flash responses in Fig. 3*A*. Average (below) and variance (above) were computed at 12 msec digitizing intervals; flash timing is shown in middle. Curve fitted to average is the Poisson eqn. (3) of Baylor *et al.* (1979), with $n = 4$, $t_{peak} = 2{\cdot}2$ sec. The relatively high base line variance was the result of DC drift. T_1, T_2 and T_3 are the time windows used in calculating the response amplitude (see Methods).

Shape of the histogram

The close agreement of the three estimates of response size supports the notion that the prominent peak in the amplitude histogram near 1 pA corresponds to occurrence of a unit electrical response. It is clear that this peak is considerably wider than the peak at 0 pA, which suggests the existence of dispersion in the event amplitude. To describe this we assume that the amplitude of the unit response is Gaussian distributed with variance σ_1^2 about its mean, a, and also that there is an independent additive 'background' noise with variance σ_0^2. The expected distribution of observed amplitudes will be the sum of Gaussian components each with mean ka,

variance $(\sigma_0^2+k\sigma_1^2)$ and with an area weighted according to the Poisson eqn. (6). Thus the probability density, $p(r)$, of a response with amplitude in the range r to $r+\mathrm{d}r$ is

$$p(r) = \sum_{k=0}^{\infty} \frac{\mathrm{e}^{-m}m^k}{k!} \frac{1}{(2\pi(\sigma_0^2+k\sigma_1^2))^{\frac{1}{2}}} \exp\left(-\frac{(r-ka)^2}{2(\sigma_0^2+k\sigma_1^2)}\right). \quad (10)$$

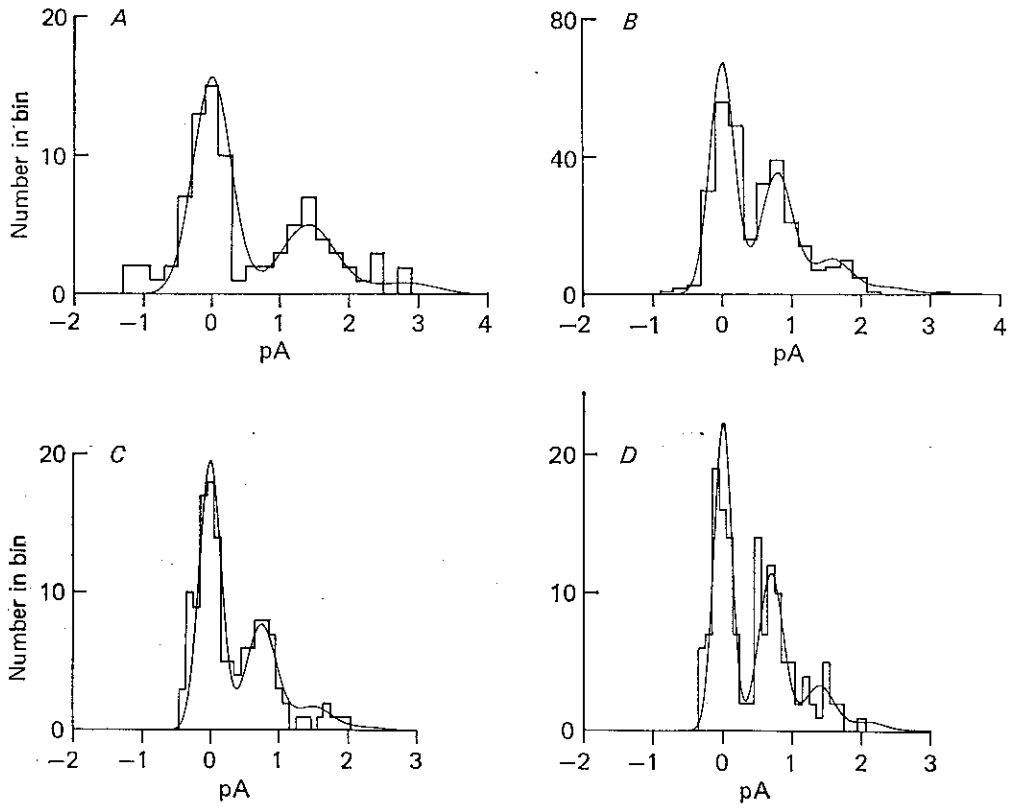

Fig. 5. Amplitude histograms of dim flash responses from four cells, plotted as in Fig. 3. See Table 1, cells 2–5 for numbers of trials and parameters used in fitting curves.

Eqn. (10) has been fitted to the histogram in Fig. 3*A* and provides a good fit. In choosing the four parameters m, a, σ_0 and σ_1 we used the value $m = 0{\cdot}53$ calculated above, and $a = 1{\cdot}2$ pA from inspection of the unit peak. The values of σ_0 and σ_1 were then varied to provide the best fit by eye, giving $\sigma_0 = 0{\cdot}15$ pA and $\sigma_1 = 0{\cdot}3$ pA. As a check the total variance expected for this choice of parameters can be calculated from a corrected form of eqn. (9) which allows for dispersion of the quantal events (see Katz & Miledi, 1972)

$$\sigma^2 = m(a^2+\sigma_1^2)+\sigma_0^2, \quad (11)$$

giving $\sigma^2 = 0{\cdot}84$ pA^2. After correction for non-linear summation (Katz & Miledi, 1972), with an expected mean of 0·64 pA ($m = 0{\cdot}53$, $a = 1{\cdot}2$ pA) and maximal response of 12 pA, this reduces to $\sigma^2 = 0{\cdot}68$ pA^2 compared with the observed value of 0·58 pA^2. The disparity may simply have resulted from the absence of some of the expected large responses because of the finite sample size.

In Fig. 3*B* the value of m has been scaled by the measured ratio of intensities to give $m = 0{\cdot}25$, while the remaining parameters are unchanged, and the curve (for fifty-two trials) provides an adequate fit in view of the small number of expected

successes. The reasonable fit to the histograms supports the notion that the outcome of any trial is a randomly distributed integral number of unit events each contributing an amplitude of roughly 1 pA.

Fig. 5 illustrates amplitude histograms from four cells at approximately this level of response; additional histograms from another cell are shown in Fig. 8. Values of the parameters estimated from eight cells are collected in Table 1. In these cells the unit response had a mean amplitude a of 0·96 pA and a standard deviation σ_1 of 0·20 pA; in addition there was an additive noise with standard deviation σ_0 of

TABLE 1. Parameters obtained in histogram fits. The parameters m, a, σ_0 and σ_1 are those used in eqn. (10) to fit the histograms. The mean number of events per trial is denoted m; for each cell a is the unit event amplitude, σ_1 its standard deviation, and σ_0 the standard deviation of the base-line noise. The ratio $(a/\sigma_1)^2$ gives the number of particles corresponding to the observed coefficient of variation of the quantal response (see Discussion)

Cell	Fig.	Trials	m	a (pA)	σ_0 (pA)	σ_1 (pA)	$(a/\sigma_1)^2$	
1	3*A*	99	0·53	1·2	0·15	0·30	16	
	3*B*	52	0·25	1·2	0·15	0·30	16	
2	5*A*	87	0·46	1·4	0·28	0·28	25	
3	5*B*	297	0·68	0·8	0·18	0·15	28	
4	5*C*	133	0·54	0·75	0·16	0·15	25	
5	5*D*	145	0·70	0·7	0·13	0·12	34	
6	8*A*	101	0·70	1·15	0·23	0·25	21	460 nm
	8*B*	149	0·49	1·15	0·23	0·25	21	580 nm
	8*C*	100	0·51	1·15	0·23	0·25	21	700 nm
7	—	314	0·80	0·7	0·17	0·17	17	
8	—	393	0·80	1·0	0·25	0·20	25	
			Mean	0·96	0·19	0·20	23	

0·19 pA. Using these values of the parameters a, σ_0 and σ_1 an investigation was made of the theoretical effect of changes in m on the shape of the histogram; it was found that the clearest separation between the zero and unit peaks occurred for values of m in the range 0·5–1·5.

In three cells for which reasonably long stable flash series were obtained, the amplitude histograms showed no sign of quantization. In several other cells short series of flashes suggested that quantization would not be observed, and the cells were not studied further. Lack of apparent quantization may have resulted from a small unit event amplitude a, or alternatively from a large standard deviation σ_0 or σ_1. Two of the three cells had 'fast' flash responses ($t_{peak} < 1$ sec), and as it was shown previously (Baylor *et al.* 1979) that this was correlated with low flash sensitivity, it seems likely that these cells may have had small unit amplitudes. Excessive variability in the quantal response (i.e. large σ_1) might have arisen for example from sensitivity differences along the outer segment (see Baylor *et al.* 1979), while excessive background noise (large σ_0) could have arisen from a continuous intrinsic 'dark noise' similar to that in turtle cones (Lamb & Simon, 1977) or from occurrence of spontaneous photon-like events at times uncorrelated with the flashes. Whatever the causes, about a third of cells failed to show obvious quantization.

Relation between unit response and photoisomerization

It is of obvious interest to determine whether the elementary electrical event is triggered by a single photoisomerization or whether the co-operative effect of several isomerizations is required. We examined this with a 'frequency of seeing' experiment similar to that performed by Hecht, Shlaer & Pirenne (1942) psychophysically, and by Fuortes & Yeandle (1964) and Scholes (1965) with intracellular recording in invertebrate photoreceptors. From several dim flash runs at various intensities histograms were constructed allowing the fraction of successes to be determined at each intensity. Fig. 6 plots the fraction of successes for one cell as a function of light intensity on a logarithmic scale.

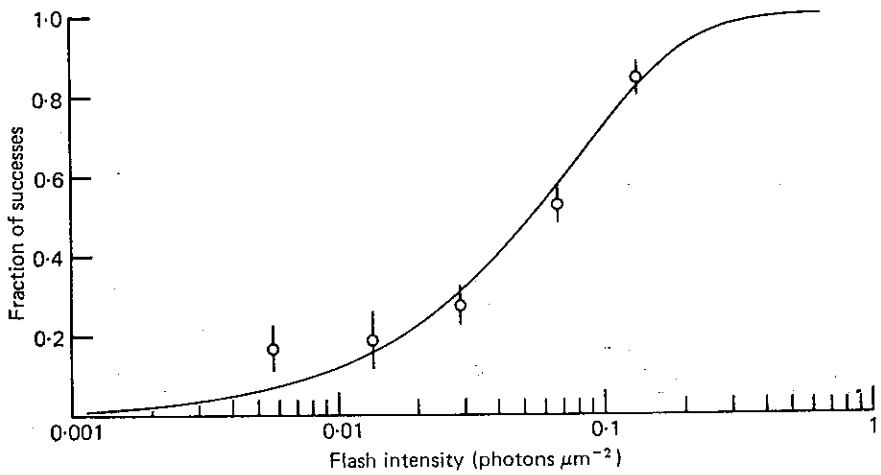

Fig. 6. 'Frequency of seeing' experiment. Fraction of responses exceeding criterion level (ordinate) at five intensities is plotted against flash intensity on a logarithmic scale. Bars are ±1 standard deviation estimated from the numbers of successes and failures. Intensities (photons μm^{-2}), and successes/trials respectively were: 0·0057, 8/47; 0·014, 6/32; 0·029, 23/83; 0·068, 67/127; 0·13, 71/84. Curve is eqn. (13) with A = 12·7 μm^2. From the outer segment diameter (6·4 μm) and length stimulated (25·5 μm), A was calculated as 10·1 μm^2 using eqn. (14).

The curve is calculated on the assumption that only a single photoisomerization is required to elicit a unit electrical response. The mean number of photoisomerizations m should be proportional to light intensity

$$m = Ai, \tag{12}$$

where i is flash intensity (photons μm^{-2}) and the constant A is the effective collecting area of the outer segment (μm^2). The probability of success p_s is then found as $1-p_0$ where p_0 in eqn. (7) is the probability of failure, so that

$$p_s = 1-e^{-Ai}. \tag{13}$$

The curve representing this equation was positioned horizontally to provide a best fit by eye to the points in Fig. 6, thus fixing the value of the area A as 12·7 μm^2. This is very close to the value of 10·1 μm^2 estimated independently from cell dimensions and known pigment density by the approximate relation

$$A = \frac{\pi d^2 l}{4} Q_{isom} f 2{\cdot}303 \alpha. \tag{14}$$

Here l is the length of outer segment stimulated by the light, d is its diameter (the stimulus being wider than the cell), Q_{isom} is the quantum efficiency of isomerization (0·67; Dartnall, 1972), and α is the specific axial pigment density (0·016 μm^{-1}; Harosi, 1975). For light polarized in the preferred direction the factor f is unity, while for unpolarized light it is reduced to 0·5 to allow for imperfect absorption of light incident normal to the axis of the outer segment. This simplified equation is restricted to the case of negligible self-screening, i.e. $2{\cdot}303\alpha d \ll 1$.

The alternate assumption that two isomerizations were required to elicit a quantal response gave a theoretical curve which was too steep to fit the points well, and which, to provide even a moderate fit, required the unreasonably large value for collecting area of almost 40 μm^2; higher co-operativities gave even poorer fits. In addition, in five other cells for which fewer intensities were tested, both the position and slope of the points were consistent with the curve for a single photoisomerization. These results provide strong evidence that each quantal response is elicited by only a single photoisomerization.

Quantum efficiency of response production

Previous spectrophotometric measurements on rhodopsin in detergent solutions have shown that absorption of a photon leads to isomerization of the absorbing molecule with a probability of 0·67 (see Dartnall, 1972). This probability is termed the quantum efficiency of isomerization, Q_{isom}. With the present technique it is possible to measure a different parameter, namely the probability, Q_{resp}, that an absorbed photon will trigger an elementary electrical response. It is defined as the ratio of the mean number of quantal responses per flash, m, to the mean number of photons absorbed per flash, ϕ_{abs}, or

$$Q_{\text{resp}} = \frac{m}{\phi_{\text{abs}}}. \tag{15}$$

ϕ_{abs} was determined from measurements of the incident photon flux per flash on the outer segment, ϕ_{inc}, and the fraction of incident light absorbed, f_{abs}, according to

$$\phi_{\text{abs}} = \phi_{\text{inc}} f_{\text{abs}}. \tag{16}$$

Details of the method are given on p. 614. An important feature was that light scatter from the small image on the outer segment did not materially affect the results, as it reduced both the measured fractional absorption, f_{abs}, and mean number of quantal responses, m, by the same amount. (A large degree of scatter was nevertheless undesirable as it would have increased the error in f_{abs}, which was measured by a difference method.)

Fig. 7 shows results which illustrate use of the method to determine the fractional absorption and quantum efficiency. The quantum photometer analog output during alternate 10 sec exposures to 520 and 580 nm light is shown in Fig. 7*C* prior to bleaching, and in Fig. 7*D* following complete bleaching of the rhodopsin by an unattenuated steady white light. (See legend for numerical counts.) The close agreement of the photon counts at the two wavelengths after bleaching (*D*) was fortuitous, but enables simple visual inspection of the pre-bleach traces (*C*) to show that transmission at 520 nm was lower before bleaching. The similarity of the readings at 580 nm before and after bleaching serves as a check that extraneous changes have

not occurred, while the 520 nm values give a measure of the absorption in rhodopsin at this wavelength. Neglecting absorption in rhodopsin photoproducts (see below), the counts before and after bleaching should be proportional respectively to the transmitted and incident fluxes on the outer segment in the unbleached state. Hence the fractional absorption is given by

$$f_{\text{abs}} = \frac{c_{\text{post}} - c_{\text{pre}}}{c_{\text{post}} - c_{\text{dark}}}, \tag{17}$$

where c_{pre}, c_{post} and c_{dark} are quantum photometer counts before and after bleaching and in darkness. In the experiment of Fig. 7 the apparent fraction of incident photons absorbed at 520 nm from the narrow slit image was $f_{\text{abs}} = 0{\cdot}119$. Because of inefficiency in the photomultiplier tube the photometer count does not represent the actual photon flux but is directly proportional to it. Assuming that 1 % of the photons passing through the outer segment elicit photometer counts, it can be shown that the test lights in C bleached much less than 1 % of the rhodopsin in the outer segment (see Methods).

The plot in Fig. 7*E* shows the results of a 'frequency of seeing' experiment performed on the cell prior to the absorption measurements. The abscissa is the mean number of photons absorbed per flash, determined from the measured values of the fractional absorption, unattenuated light intensity, flash duration, image size and neutral filter densities. The values for fraction of success as a function of photons absorbed were fitted by a curve equivalent to eqn. (13). The horizontal position of the curve gave the value of Q_{resp} as 0·50.

It proved to be technically difficult to perform entire experiments of this kind satisfactorily, as movement of the order of a few micrometers over a period of 20 min or so was unacceptable. In only four cells was suitable stability obtained, and these experiments gave quantum efficiencies of 0·50, 0·51, 0·87 and 0·87 for which the mean is $Q_{\text{resp}} = 0{\cdot}69 \pm 0{\cdot}11$ (S.E. of mean).

Correction for metarhodopsin III. In the foregoing consideration the effect of absorption by metarhodopsin III has been ignored, but in practice it may have a significant effect. From the data of Baumann (1972), Bowmaker (1973) and Baumann & Reinheimer (1974) the concentration of metarhodopsin III in frog rods is expected to reach its peak at roughly 150 sec after a bleaching flash (corrected to pH 7·8, 23 °C). Our bleaching light was a 60 sec step, and the first post-bleaching measurements were made about 30 sec after the end of the step, so that the metarhodopsin III concentration would not have reached its maximum. At the time of its peak concentration the absorbance of metarhodopsin III relative to that of rhodopsin may be estimated from Bowmaker (1973, Fig. 1*B*, $c-d$, $a-d$) as approximately 33 % at 520 nm (frog, pH 7·2, 5 °C). Assuming this value to be applicable to the toad at pH 7·8 and 23 °C then the absorption in metarhodopsin III at the time our measurements were made would have been 20–30 % of that in rhodopsin prior to the bleach. This means that the absorption changes measured at 520 nm represent only about 70–80 % of the actual absorption by rhodopsin, f_{abs}. Consequently, on the assumption that metarhodopsin is similar in frog and toad, the above value for the mean quantum efficiency of response Q_{resp} would be reduced by about 25 % to $0{\cdot}5 \pm 0{\cdot}1$.

It was unfortunate that the measurements were performed at a time near the peak of metarhodopsin III concentration, but little could be done to avoid this. It was not practical to make the measurements much earlier, and to wait for decay of the photoproduct would have required an extra 20 min or so, during which time small movements would inevitably have occurred. Equally, an increase in test wavelength would not have helped, as the absolute absorption in rhodopsin would

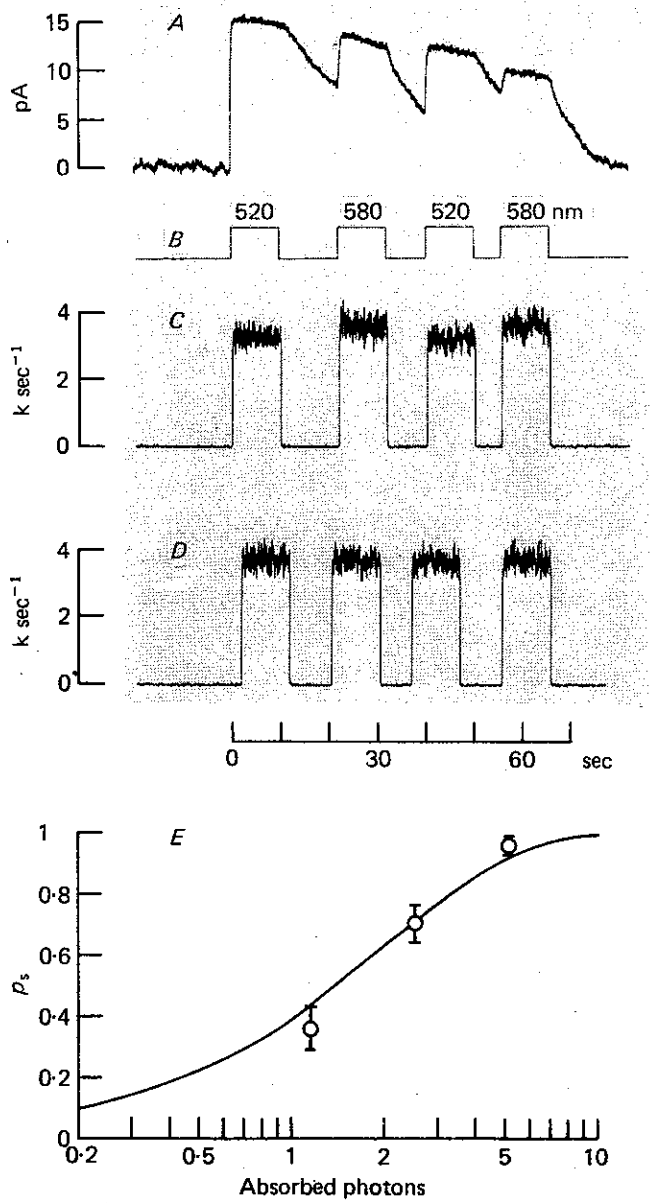

Fig. 7. Determination of quantum efficiency. *A*, membrane current of cell during 10 sec periods of 520 and 580 nm light monitored in *B*, analog output of quantum photometer for these lights before bleaching, *C*, and after complete bleaching, *D* (timing for *D* was slightly different). *E*, fraction of successful trials, p_s (determined prior to *A*–*D* at 520 nm with same stimulus geometry and same cell) is plotted against number of absorbed photons, ϕ_{abs}. Curve is analogous to eqn. (13) with $Q_{resp} = 0{\cdot}50$. Nominal image size 2·5 by 14·4 μm, centred on and parallel to long axis of outer segment; plane polarized in preferred direction. Photometer counts for the 10 sec periods were (for 520, 580, 520, 580 nm): *C* (before bleaching) 33,218, 36,296, 32,530, 36,184; *D* (after bleaching) 37,664, 37,405, 36,893, 37,402; mean dark count for 10 sec, 278.

have declined. At 580 nm, where absorption by metarhodopsin III is reduced to less than 10% of its maximum, the absorption by rhodopsin is roughly 20% of its maximum. It may be seen from the photometer counts in Fig. 7 that a small but significant increase in transmission occurred at 580 nm following the bleach, but the fractional error introduced by using such a small change would be very large. Finally, it was not practical to use a reference beam of longer wavelength than 580 nm as the condensing lens was not strictly achromatic and focusing of the very small image deteriorated.

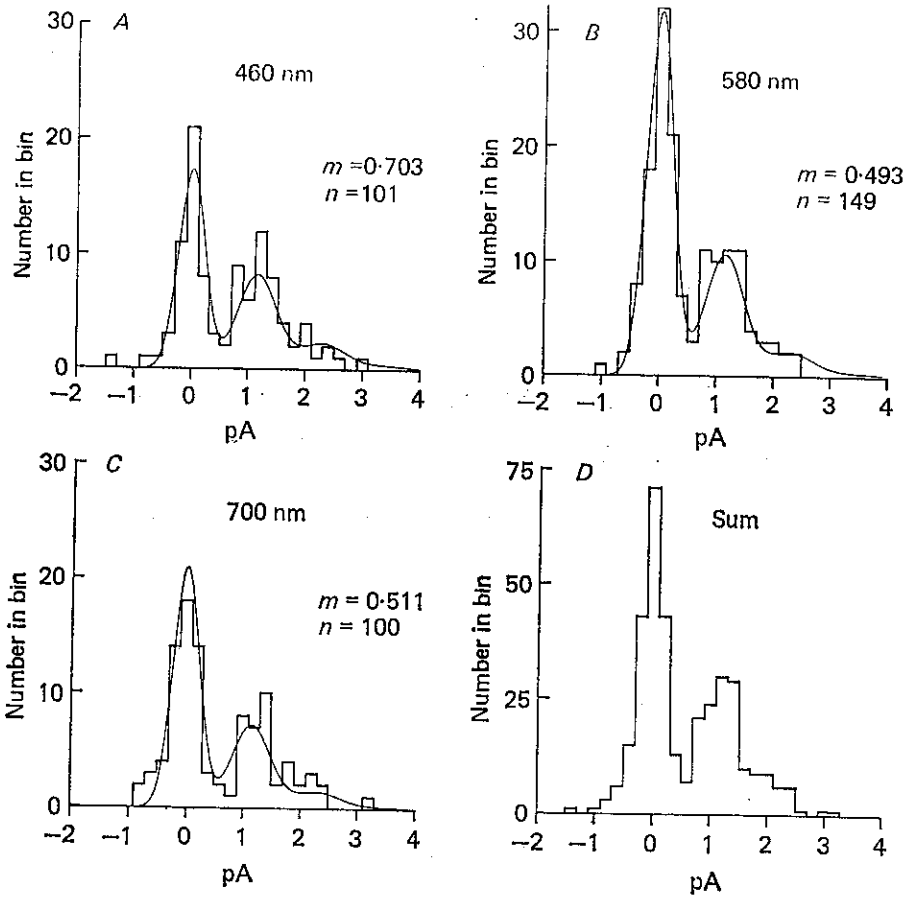

Fig. 8. 'Univariance' of the quantal response at different wavelengths: 460 nm (*A*), 580 nm (*B*), 700 nm (*C*). The histogram in *D* is the sum of the distributions in *A*, *B* and *C*. Continuous curves calculated from eqn. (10) with the following fixed parameters: $a = 1{\cdot}15$ pA, $\sigma_0 = 0{\cdot}23$ pA, $\sigma_1 = 0{\cdot}25$ pA. The mean number of events per trial, m, for each histogram was calculated by counting the number of failures and using eqn. (7); N is the number of trials. The quantum sensitivity of the cell relative to a value of unity at 500 nm was: 460 nm, 0·60; 580 nm, $9{\cdot}7 \times 10^{-2}$; 700 nm, $1{\cdot}2 \times 10^{-5}$.

Spectral univariance

Intracellular recordings from cones (Baylor & Hodgkin, 1973) showed that the linear responses to flashes of different wavelengths could be matched by suitable adjustment of the applied intensities. This result indicates that the average shape of the single photon response is independent of wavelength, but the measurements lacked the resolution required to demonstrate that the amplitude of the quantal response was also constant. Fig. 8 shows amplitude histograms from an experiment

to examine this point, in which the flash intensities at 460, 580 and 700 nm were adjusted to give average responses of similar size. It is clear that the amplitude distributions are similar, and there is no evidence that the amplitude of the quantal event differs at the three wavelengths studied. The combined amplitude histogram shown in Fig. 8*D* was used to estimate a, σ_0 and σ_1. The continuous curves were then plotted from eqn. (10) after estimating m for each histogram by counting failures.

In another experiment the flash intensities at 500 and 700 nm were each adjusted to elicit approximately quarter-maximal responses. At this mean response the photon-induced noise is expected to be maximal, and the event amplitude can be determined from the variance. This experiment showed that both the response wave form and the response variance at quarter-maximal amplitude were independent of wavelength. It is concluded that both the size and shape of the response to an absorbed photon are wavelength-invariant.

Interaction of quantal events during steady illumination

One would expect the elementary events to interact in a linear manner for small responses, so that the response to dim steady light would represent superposition of quantal events occurring randomly at a low mean rate. To investigate this we have examined the power spectrum of fluctuations resulting from dim steady illumination. In Fig. 1 the trace second from the bottom (0·068 photons μm^{-2} sec^{-1}) displayed marked fluctuations yet was close to the linear range. Its power spectral density is plotted in Fig. 9 in double logarithmic co-ordinates, and it is seen that most of the noise power is restricted to frequencies below about 0·5 Hz. At frequencies of 1–10 Hz there is a relatively flat section representing unavoidable 'white' thermal noise in the leakage resistance of the seal between pipette and cell (see p. 630), while components above 15 Hz are attenuated heavily by the 6-pole low-pass filter.

The curve in Fig. 9 is the power spectrum expected for superposition of randomly occurring events with the shape of the average flash response, and was obtained as follows. In Fig. 4 the smooth curve fitted to the average flash response of this cell is the Poisson kinetics expression with $n = 4$ stages and time to peak $t_{peak} = 2{\cdot}2$ sec (see Baylor *et al.* 1979, eqn. (3)), corresponding to four equal time constants of $\tau = 730$ msec ($\tau = t_{peak}/(n-1)$). The expected spectrum is therefore the product of n Lorentzian components each with this time constant, or

$$S(f) = \frac{S(0)}{[1+(2\pi f\tau)^2]^n}, \tag{18}$$

where $S(0)$ is the zero frequency asymptote. In Fig. 9 this curve has been scaled vertically to provide a best fit to the points and clearly represents a good description of the observed spectrum.

The vertical scaling of the curve may be checked against that predicted by the rate of photoisomerizations determined from the light intensity. For the case of a series of identical events with shape $r(t)$ occurring randomly in time at rate ν sec^{-1}, and adding linearly, the zero frequency asymptote $S(0)$ is given by

$$S(0) = 2\nu\left[\int_0^\infty r(t)\,dt\right]^2. \tag{19}$$

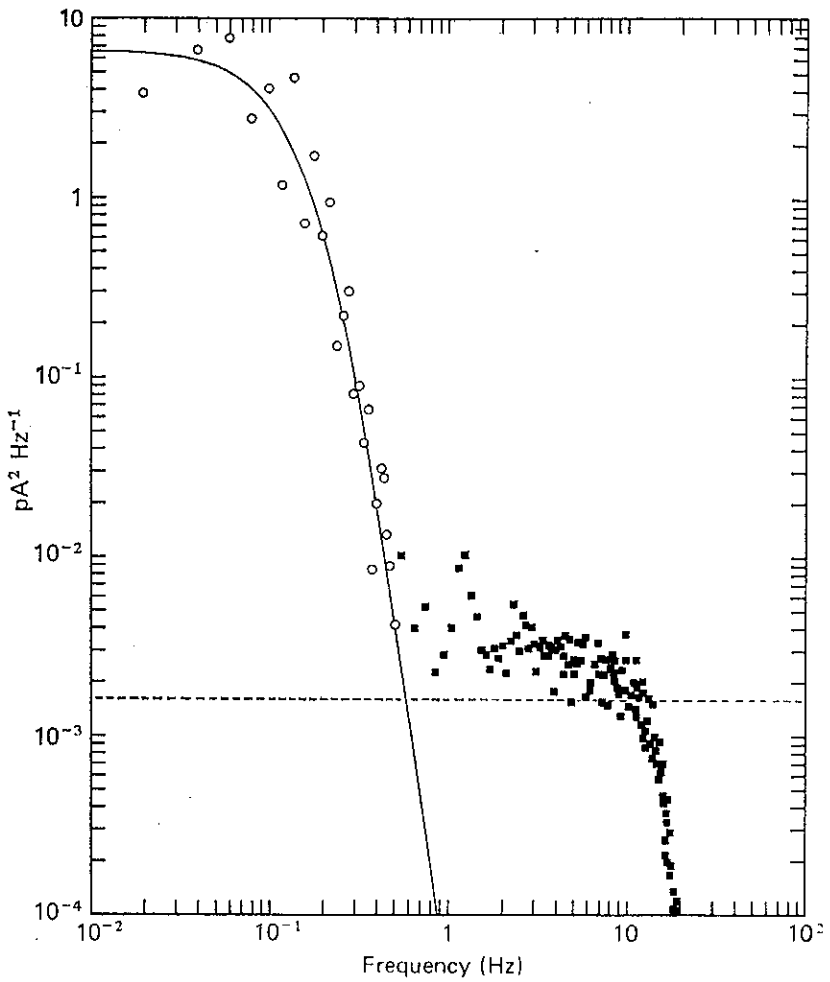

Fig. 9. Power spectral density of membrane current fluctuations in dim steady light, computed for response second from bottom in Fig. 1 (0·068 photons μm^{-2} sec^{-1}). Open symbols, raw spectral values for $f \leqslant 0{\cdot}5$ Hz; filled symbols, averages of five spectral points for $f > 0{\cdot}5$ Hz. From four records, each 2048 points at 25 msec intervals (51·2 sec); filtered by 15 Hz 6-pole low-pass filter. Continuous curve is eqn. (18) with $S(0) = 6{\cdot}6$ pA² Hz^{-1}, broken line is eqn. (21) for leakage resistance $R = 10$ MΩ.

For the Poisson kinetics discussed above with $n = 4$ stages (Baylor *et al.* 1979, eqn. (3)) this reduces to

$$S(0) = 4{\cdot}43\nu\, r_{peak}^2 t_{peak}^2, \tag{20}$$

where r_{peak} is the peak amplitude of the quantal event, and t_{peak} is the time to peak.

The cell's collecting area was estimated as $A = 16\ \mu m^2$ (from both a 'frequency of seeing' experiment and from the average flash sensitivity and unit event amplitude), so that the steady intensity of 0·068 photons μm^{-2} sec^{-1} corresponded to $\nu = 1{\cdot}1$ photoisomerizations sec^{-1}. With $t_{peak} = 2{\cdot}2$ sec and $r_{peak} = 1{\cdot}2$ pA, eqn. (20) predicted that $S(0) = 34$ pA² Hz^{-1}. This value requires correction for non-linear event summation due to the Michaelis relation between response size and light intensity. The fourth-power correction given by Katz & Miledi (1972) may not be adequate in the case of such large fluctuations as these, but for a mean response of 2·5 pA and maximal response of 12 pA, it reduces the expected zero frequency asymptote to $S(0) = 13$ pA² Hz^{-1}. Although this is somewhat larger than

the value of 6·6 $pA^2\ Hz^{-1}$ fitted in Fig. 9, it seems in reasonable agreement considering the approximations made. The discrepancy could reflect a small degree of adaptation in the steady light.

The spectral density at frequencies in the range 1–10 Hz may be compared with

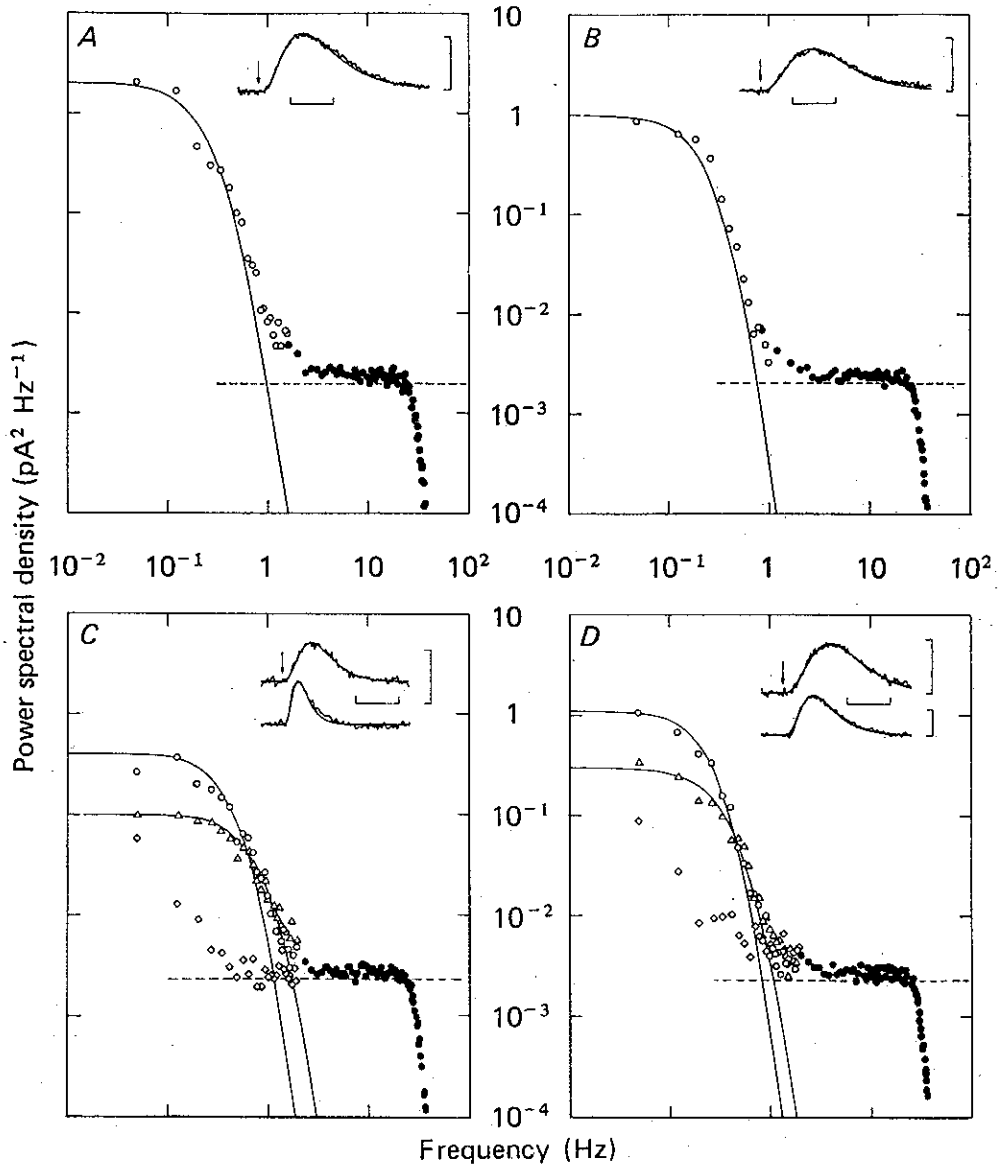

Fig. 10. Measured and predicted power spectral density during steady illumination for four cells shown in *A*, *B*, *C* and *D*. Open symbols, averages of three raw frequency points; filled symbols, averages of fifteen. ○, dim illumination (approx. 0·2 photons $\mu m^{-2}\ sec^{-1}$); △, moderate illumination (approx. 5 photons $\mu m^{-2}\ sec^{-1}$); ◇, bright illumination (approx. 500 photons $\mu m^{-2}\ sec^{-1}$). At higher frequencies only the filled circles (●) are shown. Broken line is spectral density predicted from measured leakage resistance R (eqn. (21)). Continuous curves are spectral densities (with arbitrary vertical scaling) predicted from fit to average flash responses in darkness or moderate light as shown in insets. In insets arrows mark flash timing; calibration bars: abscissa 1 sec; ordinate 1 pA (except in *B*, 0·5 pA); curves fitted by Poisson or Independence model, see Baylor *et al.* (1979) eqns. (3) and (4). See Table 2 for parameters used. Low-pass filtered at 30 Hz.

that predicted for thermal noise in the leakage resistance R between pipette and cell by the Nyquist equation

$$S_{\text{thermal}}(f) = \frac{4kT}{R}, \tag{21}$$

where k is Boltzmann's constant ($1{\cdot}38 \times 10^{-23}\,J\,°K^{-1}$) and T is absolute temperature (295 °K). For the measured leakage resistance of $R = 10$ MΩ the expected density of thermal noise is $S_{\text{thermal}}(f) = 1{\cdot}6 \times 10^{-3}\,\text{pA}^2\,\text{Hz}^{-1}$, shown by the broken horizontal line in Fig. 9. The measured spectrum in the range 1–10 Hz is somewhat higher than this, probably because of the non-ideal nature of the leakage resistance, slight changes in the seal during the experiment and components of noise introduced by the tape recorder, input amplifier, and digitizing errors.

TABLE 2. Parameters in steady light spectra. Flash response: P or I indicate that the flash responses (Fig. 4 and insets in Fig. 10) were fitted with Poisson or Independence equations respectively (see text) with n stages and with time to peak t_{peak}. The curves in Figs. 9 and 10 were obtained from these parameters (see text) with arbitrary vertical scaling, giving the values of $S(0)$. The variance of the steady response (low-pass filtered at 30 Hz) is given by σ^2. R is the pipette leakage resistance with the cell in place. Cell 1 also appears in Table 1

			Flash response			Spectrum		
Cell	Fig.	Symbol	Poisson or Independence	Stages n	t_{peak} (sec)	σ^2 (pA²)	$S(0)$ (pA² Hz⁻¹)	R (MΩ)
1	9	○, ■	P	4	2·2	0·531	6·6	10
9	10*A*	○, ●	P	4	1·0	0·465	2·0	8
10	10*B*	○, ●	P	4	1·2	0·278	1·0	8
11	10*C*	○, ●	P	4	0·68	0·201	0·4	7
		△	I	6	0·37	0·141	0·1	7
		◇	—	—	—	0·089	—	7
12	10*D*	○, ●	P	4	1·0	0·302	1·1	7
		△	I	5	0·7	0·166	0·3	7
		◇	—	—	—	0·093	—	7

Fig. 10 compares steady light power spectra from four cells with the spectra calculated from the shape of the average flash response (insets). Circles (○, ●) represent spectra in very dim steady light; the uninterrupted curves near the points plot eqn. (18) with a horizontal scale determined by the measured t_{peak} of the flash response and with a vertical scale to provide the best fit by eye. The flash responses in darkness shown in the insets are fitted by the Poisson equation with $n = 4$. In *C* and *D* the triangles (△) give spectra in steady light of moderate intensity, and the lower insets show that in these steady lights the average response to a superposed test flash was considerably faster than the flash response in darkness. Fitting the wave form of the incremental flash response gave the predicted power spectrum near each set of triangles; again the theoretical curves were arbitrarily scaled on the ordinate. The diamonds (◇) represent spectra in bright light and are dominated by thermal noise to quite low frequency; the origin of the power at the lowest frequencies is not known.

In fitting the shape of the flash responses in background light (see Table 2) it was found that the number of stages had to be increased to $n = 5$ or $n = 6$ and that the independent activation expression (Baylor, Hodgkin & Lamb, 1974, eqn. (38); Baylor *et al.* 1979, eqn. (4)) then gave an acceptable description. A possible interpretation of the altered kinetics in brighter light would be that two of the time constants governing the dark behaviour were not affected but that two shortened substantially, thus revealing the existence of one or two additional short time constants not readily detectable in darkness. The expression used for plotting the spectra for independent activation kinetics is given by Lamb & Simon, 1977, eqn. (2).

The general conclusion from the power spectral analysis presented above is that the current fluctuations in steady lights of up to at least 5 photons μm^{-2} sec^{-1} are dominated by photon-induced shot effects.

DISCUSSION

The observed amplitude of close to 1 pA for the response to a single photoisomerization is in good agreement with estimates ranging from 0·7 to 1·7 pA which can be made from previous investigations on rods (Hagins, Penn & Yoshikami, 1970; Fain, Gold & Dowling, 1976; Schwartz, 1976; Owen & Copenhagen, 1977).

The measured quantum efficiency of visual excitation of $0{\cdot}7 \pm 0{\cdot}1$, corrected to $0{\cdot}5 \pm 0{\cdot}1$ assuming frog and toad metarhodopsin III to be comparable, is not significantly different from the value of 0·67 calculated by Dartnall (1972) for the quantum efficiency of isomerization of rhodopsin in solution. This similarity suggests that the over-all efficiency of excitation may be limited by the first photochemical step, so that when a pigment molecule is isomerized an electrical response occurs with high probability.

In confirmation of the assumption of 'univariance' (Naka & Rushton, 1966), single photon effects were found to be independent of wavelength in the range 460–700 nm.

Taking the driving potential on the light-sensitive conductance to be about 40 mV in darkness, the quantal current of 1 pA corresponds to a conductance decrease of 3×10^{-11} *S*. This is close to the conductance of a single acetylcholine-sensitive channel at the neuromuscular junction (Katz & Miledi, 1972; Anderson & Stevens, 1973; Neher & Sakmann, 1976). An ACh channel exhibits abrupt transitions between open and closed states, and the lifetime of the open state is an exponentially distributed random variable with a mean of about 1 msec. A single photon instead triggers an event with a rounded stereotyped shape and a duration of a few seconds. This characteristic shape, and the size of the quantal event, have several implications for the mechanism by which the response is generated.

Assuming that the light-sensitive channels have only open and closed states, with instantaneous transitions between states, the rounded form of a single photon effect could come about in one of two ways. A photoisomerization could block a large number of channels, each with a conductance much less than 3×10^{-11} *S*. Alternatively, if channels rapidly fluctuate between the two states, a photoisomerization might modify the mean time spent in either state, so that the average response recorded with restricted bandwidth would be smooth. In either case the number of

channel-blocking particles released by a photoisomerization must be relatively large to account for the small degree of variation in quantal response amplitude.

In Table 1 the mean amplitude of the quantal response is 0·96 pA and its standard deviation is 0·20 pA, giving a coefficient of variation (*c.v.* = σ_1/a) of 0·21. Now if the quantal response, at its peak, is mediated by the blocking action of a mean number z_{peak} of transmitter molecules, and if the actual number is a Poisson-distributed random variable, then the coefficient of variation will be related to z_{peak} by

$$z_{peak} = (c.v.)^{-2} = \left(\frac{a}{\sigma_1}\right)^2, \tag{22}$$

giving $z_{peak} = 24$. However, the total number z_{total} of particles contributing to the response over its entire time course will be considerably larger than the number acting at the peak. It may be shown that z_{total} is given by

$$z_{total} = z_{peak}\frac{t_1}{\tau_z}, \tag{23}$$

where t_1 is the integration time of the response (see Baylor & Hodgkin, 1973) and τ_z is the mean time each particle exists in the active (blocking) state. For the Poisson kinetics with $n = 4$ used to fit the response shape, the factor t_1/τ_z is approximately 4·5 so that the total number of particles contributing to the single photon response is in excess of 100.

The total number of blocking particles released as a result of a single isomerization may be considerably larger than this for a number of reasons. First, it is unlikely that all particles released from the disk reach the vicinity of the plasma membrane, or that all those reaching the membrane bind to light-sensitive channels. Secondly, it is possible that the number above represents the amount of a precursor substance, each molecule of which leads to the release of a large number of the blocking molecules. Thirdly, the value of $\sigma_1 = 0{\cdot}20$ pA is an upper estimate of the dispersion in quantal amplitude attributable to the transduction process *per se*, because a component of the observed dispersion probably arises from variations in response properties at different positions along the outer segment (see Baylor *et al.* 1979).

On the other hand, if the light-sensitive channels in a local region of the outer segment were partly saturated by blocking particles during the response to a single photon, then the resulting dispersion would be less than predicted by eqn. (22) and the number of particles would be over-estimated. An over-estimate might also result if the interaction between particles and channels were not a rapidly reversible equilibrium binding, as implicitly assumed above, but instead constituted one of the delays in the response wave form.

Several authors have suggested that a diffusion process may limit the initial rise of the visual response to light (Ives, 1922; Cone, 1964; Rushton, 1965; Kelly, 1971). If a significant component of the delay arose from radial diffusion of internal transmitter from the site of absorption in a disk to the outer plasma membrane, then the form of the quantal event should depend on the radial position at which the isomerization occurred. In particular, absorption of a photon near the perimeter would give a large response with little delay, while absorption near the centre would give a smaller and slower response. In our experiments a given cell's quantal responses

varied only slightly in time course and amplitude between trials. This, together with the points mentioned by Baylor *et al.* (1974), suggests that diffusion is not a major source of delay in the photoresponse, although it certainly must make some contribution.

We wish to thank Mr G. Kuhn for excellent technical assistance, Professor A. L. Hodgkin for suggesting the spectral univariance experiment and Dr V. Torre for suggestions relating to the number of transmitter particles. This work was supported by grant EY-01543 from the National Eye Institute, USPHS, by grants from the Sloan and Sinsheimer Foundations, and by a Bank of America–Giannini Fellowship to K.-W. Y.

REFERENCES

ANDERSON, C. R. & STEVENS, C. F. (1973). Voltage clamp analysis of acetylcholine-produced end-plate current fluctuations at frog neuromuscular junction. *J. Physiol.* **235**, 655–691.

BAUMANN, C. (1972). Kinetics of slow thermal reactions during the bleaching of rhodopsin in the perfused frog retina. *J. Physiol.* **222**, 643–663.

BAUMANN, C. & REINHEIMER, R. (1974). Temperature dependence of slow thermal reactions during the bleaching of rhodopsin in the frog retina. *Biochemistry and Physiology of Visual Pigments*, ed. LANGER, H., pp. 89–99. New York: Springer.

BAYLOR, D. A. & FUORTES, M. G. F. (1970). Electrical responses of single cones in the retina of the turtle. *J. Physiol.* **207**, 77–92.

BAYLOR, D. A. & HODGKIN, A. L. (1973). Detection and resolution of visual stimuli by turtle photoreceptors. *J. Physiol.* **234**, 163–198.

BAYLOR, D. A., HODGKIN, A. L. & LAMB, T. D. (1974). The electrical response of turtle cones to flashes and steps of light. *J. Physiol.* **242**, 685–727.

BAYLOR, D. A., LAMB, T. D. & YAU, K.-W. (1979). The membrane current of single rod outer segments. *J. Physiol.* **288**, 589–611.

BENDAT, J. S. & PIERSOL, A. G. (1971). *Random Data: Analysis and Measurement Procedures.* New York: Wiley.

BOWMAKER, J. K. (1973). The photoproducts of retinal-based visual pigments *in situ:* a contrast between *Rana pipiens* and *Gekko gekko*. *Vision Res.* **13**, 1227–1240.

CONE, R. A. (1964). The rat electroretinogram. II. Bloch's law and the latency mechanism of the b-wave. *J. gen. Physiol.* **47**, 1107–1116.

DARTNALL, H. J. A. (1972). Photosensitivity. In *Photochemistry of Vision*, ed. DARTNALL, H. J. A., pp. 122–145. New York: Springer.

DAVENPORT, W. B. & ROOT, W. L. (1958). *An Introduction to the Theory of Random Signals and Noise.* New York: McGraw-Hill.

FAIN, G. L. (1975). Quantum sensitivity of rods in the toad retina. *Science, N.Y.* **187**, 838–841.

FAIN, G. L., GOLD, G. H. & DOWLING, J. E. (1976). Receptor coupling in the toad retina. *Cold Spring Harb. Symp. quant. Biol.* **40**, 547–561.

FUORTES, M. G. F. & YEANDLE, S. (1964). Probability of occurrence of discrete potential waves in the eye of *Limulus*. *J. gen. Physiol.* **47**, 443–463.

HAGINS, W. A., PENN, R. D. & YOSHIKAMI, S. (1970). Dark current and photocurrent in retinal rods. *Biophys. J.* **10**, 380–412.

HAROSI, F. I. (1975). Absorption spectra and linear dichroism of some amphibian photoreceptors. *J. gen. Physiol.* **66**, 357–382.

HECHT, S., SHLAER, S. & PIRENNE, M. H. (1942). Energy, quanta, and vision. *J. gen. Physiol.* **25**, 819–840.

IVES, H. E. (1922). A theory of intermittent vision. *J. opt. Soc. Am.* **6**, 343–361.

KATZ, B. & MILEDI, R. (1972). The statistical nature of the acetylcholine potential and its molecular components. *J. Physiol.* **224**, 665–699.

KELLY, D. H. (1971). Theory of flicker and transient responses. I. Uniform fields. *J. opt. Soc. Am.* **61**, 537–546.

LAMB, T. D. & SIMON, E. J. (1977). Analysis of electrical noise in turtle cones. *J. Physiol.* **272**, 435–468.

NAKA, K. I. & RUSHTON, W. A. H. (1966). S-potentials from colour units in the retina of fish (*Cyprinidae*). *J. Physiol.* **185**, 536–555.

NEHER, E. & SAKMANN, B. (1976). Single-channel currents recorded from membrane of denervated frog muscle fibres. *Nature, Lond.* **260**, 799–802.

OWEN, W. G. & COPENHAGEN, D. R. (1977). Characteristics of the electrical coupling between rods in the turtle retina. In *Vertebrate Photoreception*, ed. BARLOW, H. B. & FATT, P., pp. 169–190. New York: Academic Press.

RUSHTON, W. A. H. (1965). The Ferrier Lecture, 1962. Visual adaptation. *Proc. R. Soc.* B **162**, 20–46.

SCHOLES, J. (1965). Discontinuity of the excitation process in locust visual cells. *Cold Spring Harb. Symp. quant. Biol.* **40**, 517–527.

SCHWARTZ, E. A. (1975). Rod–rod interaction in the retina of the turtle. *J. Physiol.* **246**, 617–638.

SCHWARTZ, E. A. (1976). Electrical properties of the rod syncytium in the retina of the turtle. *J. Physiol.* **257**, 379–406.

YAU, K.-W., LAMB, T. D. & BAYLOR, D. A. (1977). Light-induced fluctuations in membrane current of single toad rod outer segments. *Nature, Lond.* **269**, 78–80.